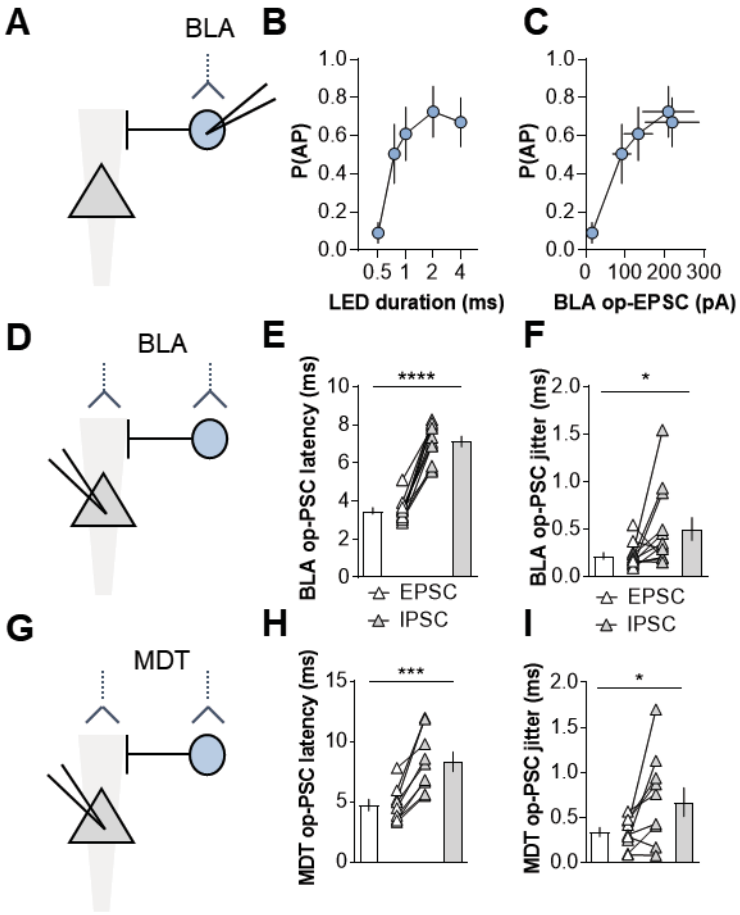

Figure S1. Related to Figure 2, BLA and MDT inputs to PFC drive feedforward inhibition.

(A) ChR2 was expressed within the BLA by viral-mediated gene transfer and recordings were made from SST-INs. **(B)** Optical stimulation of BLA terminals readily elicits SST-IN action potentials (APs) with high probability. n/N = 7/4 cells/mice. **(C)** BLA op-EPSCs as small as 100 pA readily elicit APs. n/N = 7/4 cells/mice. **(D)** ChR2 was expressed within the BLA and recordings were made from pyramidal cells. **(E)** Relative to EPSCs, BLA-driven IPSCs displayed longer onset latency (7.1±0.3 vs 3.5±0.2ms; t_{11}=12.76, ****:p<0.0001, paired t-test) and **(F)** jitter (0.50±0.12 vs 0.21±0.04ms; t_{11}=2.21, *:p<0.05, paired t-test). n/N = 12/4 **(G)** ChR2 was expressed within the MDT and recordings were made from pyramidal cells. **(H)** MDT-driven IPSCs displayed longer onset latency (8.3±0.8 vs 4.8±0.5ms; t_8=6.24, ***:p<0.001, paired t-test) and **(I)** a greater jitter (0.67±0.16 vs 0.34±0.05ms; t_9=2.3, p<0.05, paired t-test) than EPSCs. n/N = 9-10/3.

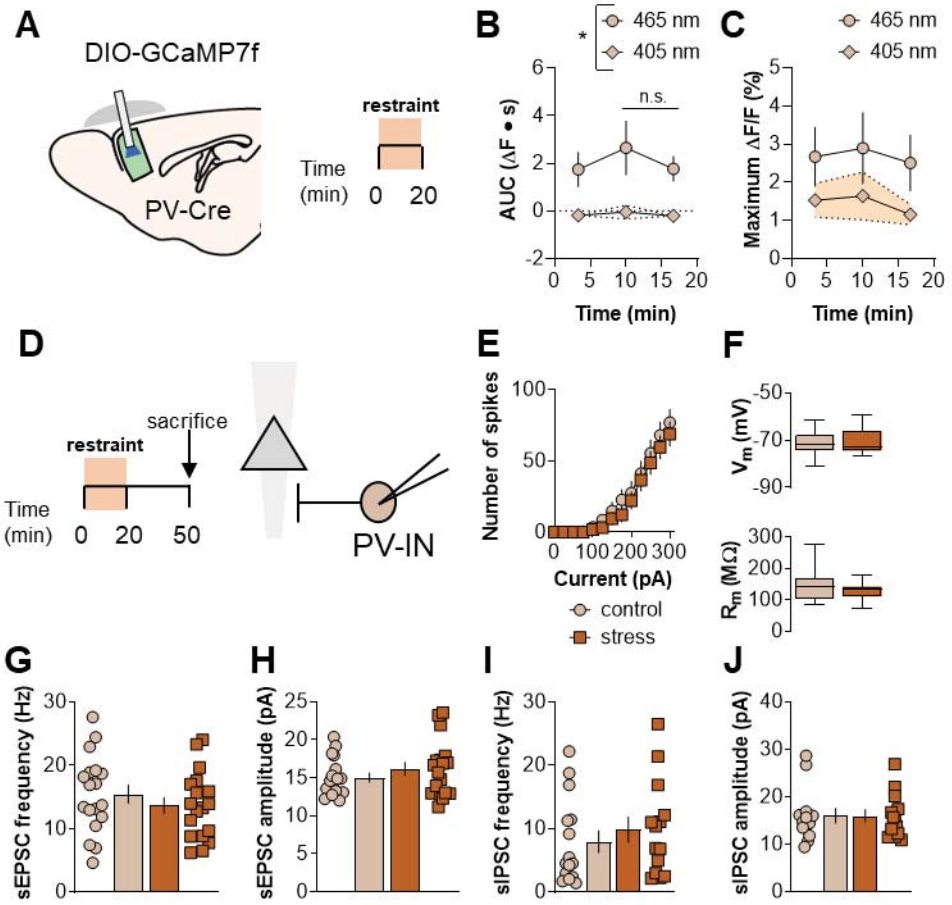

Figure S2. Related to Figure 3, Parvalbumin-expressing interneuron (PV-IN) function does not adapt during acute stress. (A) Schematic displaying viral-assisted approach to express GCaMP7f in PV-INs. A virus promoting the expression of a double-inverted open (DIO) reading frame of GCaMP7f was delivered to the PFC of PV-Cre mice and chronically indwelling fiberoptic cannulas were implanted. After 4 weeks recovery, animals underwent 20 minutes restraint stress while interneuron calcium mobilization was measured via fiber photometry. **(B)** PV-GCaMP Ca^{2+}-dependent signals (465-nm) were readily detected following struggling episodes, but their magnitude assessed by the area under the curve (AUC) did not change during a single exposure to restraint stress (RM Two-way ANOVA time x wavelength interaction: $F_{2,10}$=1.1, n.s.; main effect of wavelength: $F_{1,5}$=9.8, $p<0.03$). N=6 mice. Fluorescent signals on the Ca^{2+}-independent isobestic control channel (405-nm) were not readily detected following

struggling episodes. **(C)** The maximum increase in PV-GCaMP fluorescence locked to struggling episodes was not different than that on the isobestic control channel (RM Two-way ANOVA time x wavelength interaction: $F_{2,10}$=1.1, n.s.; main effect of wavelength: $F_{1,5}$=3.1, n.s.). N=6. **(D)** Mice were sacrificed for whole-cell electrophysiology 30 minutes following a single exposure to restraint stress. Recordings were made from PV-INs with soma in layer 5 PFC. **(E)** Restraint stress did not affect the resting membrane potential (V_m) or membrane resistance (R_m) in PV-INs. n/N = 20-23/4 cells/mice. **(F)** Current-evoked spiking was not different in PV-INs from mice in the control and restraint stress groups. n/N = 20-23/4. **(G)** sEPSC amplitude in PV-INs was not different between control and restraint stress groups n/N = 17-18/4. **(H)** Acute stress did not alter PV-IN spontaneous excitatory postsynaptic current (sEPSC) frequency n/N = 17-18/4. **(I)** Acute stress did not alter PV-IN spontaneous inhibitory postsynaptic current (sIPSC) frequency n/N = 13/4. **(J)** sIPSC amplitude in PV-INs was not different between control and restraint stress groups n/N = 14-15/4.

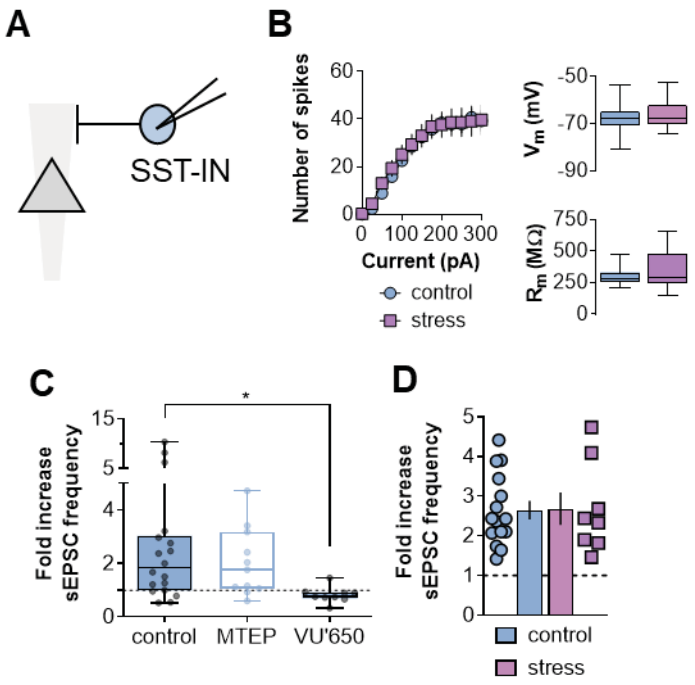

Figure S3. Related to Figure 3, Stress does not alter SST-IN intrinsic physiology or acute actions of $mGlu_1$ receptors. (A) Left, Recordings from fluorescent labeled SST-INs were made following restraint stress and in control mice. **(B)** Left, Current-evoked spiking was not different in SST-INs from mice in the control and stress groups. Right, Restraint stress did not affect the resting membrane potential (V_m) or membrane resistance (R_m) in SST-INs. n/N = 17-24/6-9 cells/mice. **(C)** During acute application, DHPG (100μM, 10min) increased the frequency of sEPSCs onto SST-INs (2.8±0.65 fold). The increase in sEPSC frequency was blocked by the $mGlu_1$ NAM VU'650 (10μM) but not the $mGlu_5$ NAM MTEP (3μM) (One-way ANOVA main effect of NAM: $F_{2,35}$=11.4, p<0.08; *:p<0.05, Sidak test). n/N=9-18/4-7. **(D)** DHPG-induced increases in sEPSC frequency were not different between SST-INs from the control and restraint stress groups. n/N=8-15/6-7.

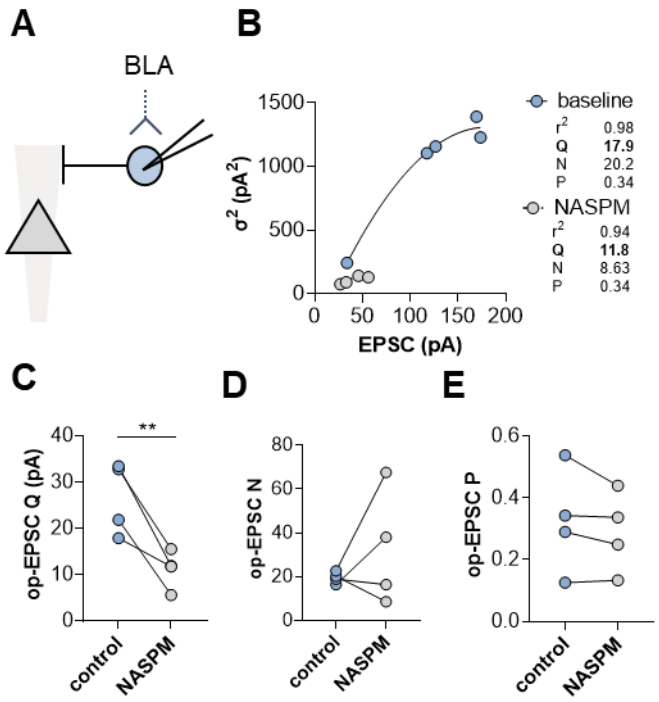

Figure S4. Related to Figure 5, Selective reduction in BLA op-EPSC Q following NASPM administration. (A) ChR2 was expressed in the BLA and recordings were made from layer 5 SST-INs in PL PFC. **(B)** Representative MPFA experiment. For each cell, op-EPSC amplitude and standard deviation (σ) were obtained across a range of light stimulation durations. A quadratic equation was fit to the op-EPSC amplitude and variance (σ^2) at baseline and in the presence of NASPM (200μM, 15min). The quantal size (Q), number of synapses (N), and glutamate release probability (P), can be derived from the curve fit parameters. **(C)** NASPM reduced quantal size on SST-INs (11.1±3.2 vs 26.5±3.9pA; t_3=4.7, $p<0.02$, t-test). n/N = 4/3 cells/mice. **(D)** NASPM did not affect N at BLA inputs onto SST-INs. **(E)** P from BLA to SST-INs was not affected by NASPM.

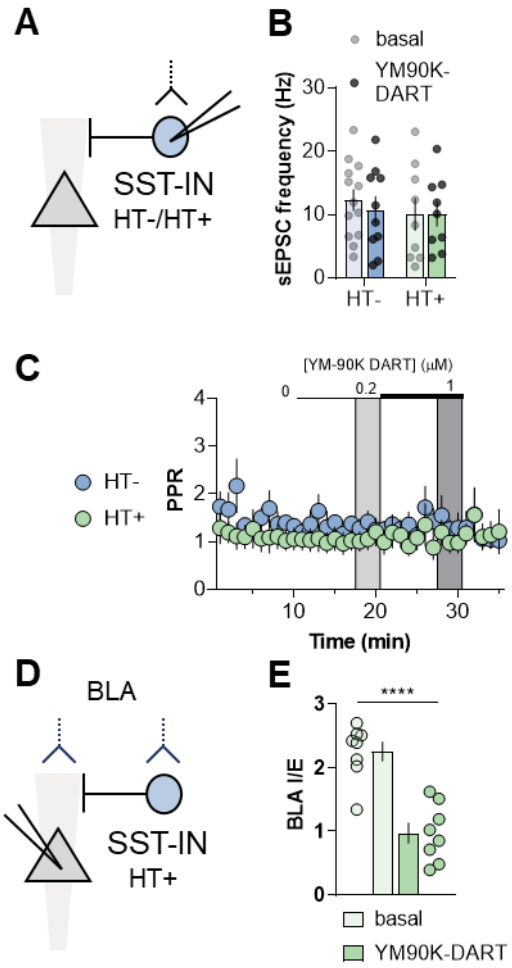

Figure S5. Related to Figure 5, YM90K DART administration attenuates BLA-elicited feedforward inhibition without affecting presynaptic release parameters on SST-INs . (A) DART was deployed by viral-mediated expression of the HaloTag protein (HT+), or an inactive mutant variant (HT-), selectively in PFC SST-INs. Both constructs also expressed tdTomato to allow for visualization and cellular targeting. **(B)** No effect of YM90K DART application on sEPSC frequency in either HT- or HT+ SST-INs. n/N=9-13/3-4 cells/mice**.** (**C)** The AMPA receptor antagonist YM90K DART did not affect PPR of electrically evoked EPSCs on SST-INs. n/N=4-5/3-4**. (D)** HT+ was expressed in PFC SST-INs, ChR2 was expressed in BLA terminals, and BLA op-EPSCs and disynaptic op-IPSCs were recorded from pyramidal cells. **(E)** The amplitude ratio of BLA op-IPSCs relative to op-EPSCs (I/E) was decreased by YM90K-DART (2.3 ± 0.2 vs 1.0 ± 0.2; t_{14}=5.83, ****:p<0.0001, t-test). n/N=8/3**.**

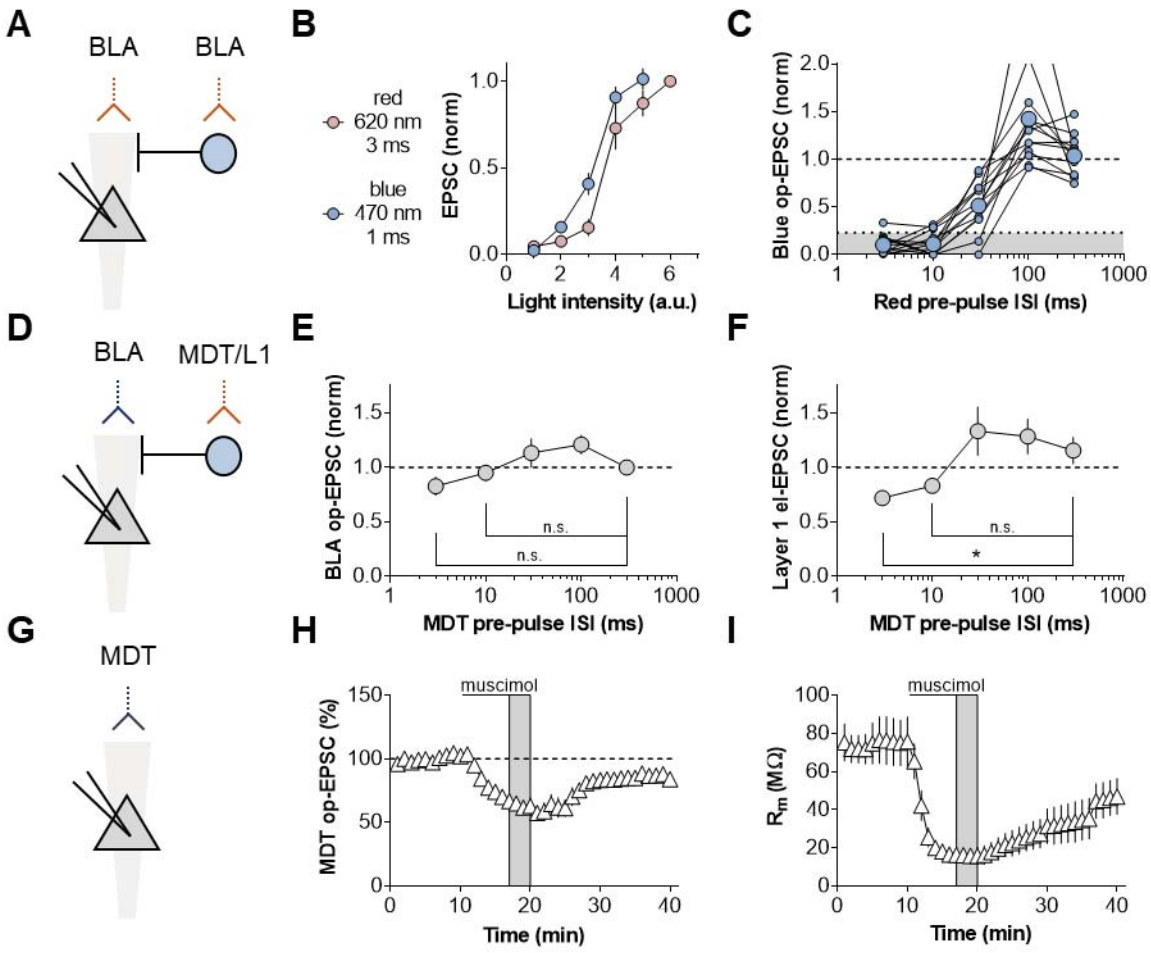

Figure S6. Related to Figure 5, Control experiments supporting BLA-driven heterosynaptic shunting inhibition. (A) Chrimson was expressed in the BLA without any expression of ChR2. **(B)** Stimulation with either blue (470nm, 1ms) or red (620nm, 3ms) light readily evoked EPSCs in PFC pyramidal cells. n/N = 8/3 cells/mice. For experiments utilizing both Chrimson and ChR2, red light stimulation was saturating, and blue light was kept below 2 a.u. for experiments in the main body of the manuscript. **(C)** The intensity of blue light was increased to 4-5 a.u. to evoke comparable EPSCs as red. Short-latency red light pre-pulses (3-10ms) prevented any subsequent BLA op-EPSCs evoked via blue light stimulation, suggesting spectral overlap is unlikely to contribute to blue light EPSCs in dual opsin experiments. n/N = 12/4. **(D)** A dual opsin strategy was employed to evaluate interactions between BLA and MDT inputs on isolated pyramidal cells. The red-shifted opsin Chrimson was expressed in the MDT

and ChR2 was expressed in the BLA. Red light stimulation preceded blue light stimulation. **(E)** Prior stimulation of MDT terminals did not decrease the amplitude of subsequent BLA op-EPSCs (RM One-way ANOVA main effect of ISI: $F_{4,44}$=5.1, p<0.01; n.s. Sidak tests vs 300ms). n/N=12/3 cells/mice. **(F)** Prior stimulation of MDT terminals decreased the amplitude of EPSCs evoked with L1 electrical stimulation 3-ms later but not at 10-ms pre-pulse ISIs associated with SST-IN disynaptic inhibition. (RM One-way ANOVA main effect of ISI: $F_{4,36}$=6.76, p<0.001; *:p<0.05. Sidak tests vs 300ms). n/N=10/5 cells/mice. **(G)** ChR2 was expressed in the MDT and recordings were made from pyramidal cells. **(H)** The $GABA_A$ receptor agonist muscimol (10μM, 10min) depressed the amplitude of MDT op-EPSCs (63.2±6.2% baseline) **(I)** concomitant with a reduction in R_m (21.6±5.8% baseline). n/N = 5/2.

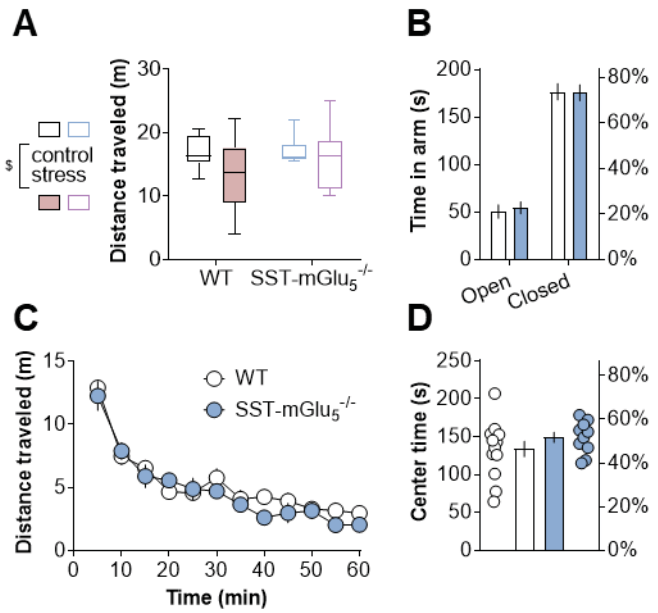

Figure S7. Related to Figure 8, WT and SST-mGlu$_5^{-/-}$ mice display comparable locomotor behavior. (A) Trend decrease in locomotor activity in the Y-maze apparatus following restraint stress, but no main effect of genotype or interaction (Two-way ANOVA stress x KO interaction: $F_{1,38}$=1.0, n.s.; main effect of stress: $F_{1,38}$=6.1, $:p<0.07). N=10-12 mice per group. **(B)** No genotypic difference was detected in the proportion of time spent in the open arms of an elevated zero-maze. N=10-13. **(C)** SST mGlu$_5^{-/-}$ mice displayed typical locomotor activity in a novel environment. N=10-13. **(D)** No difference in the proportion of time spent in the center of the open field during the first 5 minutes of the test. N=10-13.

Supplemental Table 1. Related to Figure 1, Membrane physiology parameters characterizing LTS SST-INs

Parameter	Unit	Cell type	Mean	SEM	t(32)	p
V_m	mV	LTS	-63.3	1.6	4.7	****
		FSL	-76.3	1.2		
R_m	MΩ	LTS	411	24	5.9	****
		FSL	171	18		
rebound sag	-	LTS	0.063	0.008	2.6	*
		FSL	0.027	0.005		
rheobase	pA	LTS	30	3	6.9	****
		FSL	139	27		
max frequency	Hz	LTS	44	4	8.7	****
		FSL	119	9		

FSL, fast-spiking-like; LTS, low-threshold-spiking; R_m, membrane resistance; V_m, resting membrane potential

Supplemental Table 2. Related to Figures 1, 2, 3, 5, 6, 7;
Amplitudes of EPSCs for normalized data sets

Cell type	Input	Panel	Condition	Mean	SEM	n cells	N ♀	N ♂
SST-IN	electrical	1E	K-gluconate	86	19	12	6	5
		1F	VU'650	51	14	8	3	4
			MTEP	54	15	8	3	4
		1J	BAPTA	46	7	5	3	1
		3I	control	52	13	12	4	6
			stress	89	25	8	2	2
		3L	control	113	20	7	2	4
			stress	103	21	7	1	4
		5E	HT-	91	19	4	0	3
			HT+	75	9	5	0	4
		7D	WT	103	32	6	1	2
			KO	113	16	5	1	1
	BLA	2D	-	150	36	4	1	3
		2G	control	168	54	8	2	3
			MTEP	245	70	5	2	1
	MDT	2D	-	302	91	5	1	3
		2H	-	201	92	7	1	2

				EPSC (pA)		IPSC (pA)				
	Input	Panel	Condition	Mean	SEM	Mean	SEM	n cells	N ♀	N ♂
pyramidal cell	electrical	5C / 5L	K-gluconate	210	40	-	-	9	2	2
		5C	picrotoxin	388	158	-	-	8	2	1
		5I	basal	191	69	-	-	8	3	0
			YM90K-DART	247	89	-	-	7		
		S4	MDT-elec study	162	42			11	1	4
	BLA	2K	basal	469	97	449	97	9	0	3
			post DHPG	391	41	728	132	9	0	3
		5C / 5L	K-gluconate	224	30	-	-	9	2	2
		5C	picrotoxin	216	50	-	-	8	2	1
		5K	K-gluconate	271	47	-	-	16	2	3
			picrotoxin	206	44	-	-	5	2	0
		5L	stress	190	36	-	-	10	2	1
		6F / 6H	control	224	42	340	70	8	0	3
			stress	295	51	1089	190	8	0	3
		S6	HT+ baseline	317	52	664	157	9	3	0
			HT+ YM90-K	340	72	352	100	8		
	MDT	2L	basal	334	98	918	244	6	1	3
			post DHPG	629	174	1276	194	8	1	3
		5K / 5L	control	175	28	-	-	16	2	3
			stress	304	125	-	-	10	2	1
		6K / 6M	control	241	32	871	166	10	0	3
			stress	246	60	893	244	10	0	3
		S4	MDT-elec study	222	34	-	-	11	1	4